

SUPERCOOLING WATER IN CYLINDRICAL CAPSULES¹

J. J. Milón² G. and S. L. Braga^{2,3}

¹ Paper presented at the Fifteenth Symposium on Thermophysical Properties, June 22-27, 2003, Boulder, Colorado, U.S.A.

² Department of Mechanical Engineering. Pontifical Catholic University of Rio de Janeiro. CEP 22453-900 – Rio de Janeiro, RJ, Brazil

³ Correspondence should be addressed to - E-mail: slbraga@mec.puc-rio.br

ABSTRACT

An experimental apparatus was developed to investigate the supercooling phenomenon of water inside cylindrical capsules used for cold storage process. The transfer fluid (TF), is a water-alcohol mixture, controlled by a constant temperature bath (CTB). Temperatures varying with time are measured inside and outside the capsule. Cylinders with internal diameter and thickness of 45 mm and 1.5 mm, respectively, were made from four different materials: Acrylic, PVC, Brass and Aluminum. The supercooling period of the water and the nucleation temperature were investigated for different transfer fluid temperatures. The supercooling and nucleation probabilities are shown as a function of the transfer fluid temperature for the four different materials.

KEY WORDS: air conditioning, nucleation, phase change, supercooling, refrigeration, thermal storage.

Nomenclature

T	temperature, [°C]
T _{TF}	transfer fluid temperature, [°C]
T _{di}	maximum density temperature, [°C]
T ₀	initial temperature, [°C]
T _m	phase change temperature, [°C]
T _n	nucleation temperature, [°C]
SD	supercooling degree, [°C]
N _S	supercooling probability, []
N _F	nucleation probability, []
CR	cooling rate, [°C min ⁻¹]

Convention

PCM	phase change material
Δt	duration of the supercooled state
TF	transfer fluid
CTB	constant temperature bath
PVC	polyvinyl chloride
PID	proportional, integral and derivative control

1. INTRODUCTION

The thermal storage for refrigeration systems is an important concept of many energy conservation programs. Water is widely used as the phase-change material (PCM) due to its advantages: high value in latent heat, stable chemical properties, low cost and easy acquisition, no environmental pollution concern, and compatibility with the materials used in air-conditioning equipment. However, there are a few disadvantages in using water as PCM. Two of the most serious problems encountered are the supercooling phenomenon and the density inversion occurring in the water solidification during the thermal storage cooling process.

When the water is cooled in an enclosed container, freezing does not occur at its freezing point (0°C) at atmospheric pressure. Instead, it is normally cooled below 0°C before ice nucleation happens. Supercooled water refers to a state of metastable liquid even though the water temperature is below its freezing temperature. The metastable state ends when ice nucleation occurs and the thin plate-like crystal of dendritic ice grows into the supercooled region of water. During the dendritic ice growth process, latent heat is released from the dendritic ice and consumed by supercooled water. At the end of the growth process, the temperature of the water will return to its freezing point (0°C). If the metastable state exists and remains during the thermal storage process, thermal energy can only be stored in the form of sensible energy. In this case, the storage capacity is strongly reduced. Because of this, it is very important to prevent the occurrence of the supercooling and to acquire precise knowledge from the water supercooling phenomenon during a thermal storage process.

There are several studies about the solidification of water: Chen et al. (1) studied the numerical and experimental method to analyze the influence of nucleation agents in the water solidification process inside cylindrical copper capsules of different sizes. Yoon et al. (2) studied experimentally the freezing phenomenon of saturated water within the supercooled region in a horizontal circular cylinder using the holographic real time interferometry technique. Milón and Braga (3) studied the phenomenon of supercooling in spherical capsules of different diameters and determined the parameters that influence this phenomenon appearance.

The present work studies experimentally the supercooling phenomenon inside capsules with perfectly cylindrical geometry made from different materials.

1.1 SUPERCOOLING IN CAPSULES

For a typical stable thermodynamic water cooling process, the temperature variation versus time is presented in Fig. 1. The solidification starts in d' and finishes in f, without supercooling. The isothermal phase change process is evident. Fig. 2 presents four different cooling processes: (I) Supercooling, nucleation and evident phase change; (II) Supercooling, nucleation and no evident phase change; (III) Hypercooling and (IV) Supercooling without nucleation. For supercooled water with nucleation, the completion of freezing can be divided into four stages, as shown in Fig. 2 (except in case IV).

The first stage involves the process from the beginning of cooling, from the initial temperature T_i to the metastable state, before the occurrence of nucleation, passing through the maximum density effect, where the temperature inside the capsule is near T_{di} . This stage is called the sensible heat thermal storage process. In Fig.2: (a) water in a stable liquid state and (b) water in a metastable liquid state. T_m and T_n represent the

freezing temperature and the nucleation temperature of water, respectively, then the supercooling degree SD is defined as $(T_m - T_n)$. The second stage is the process from the occurrence of nucleation to the completion of dendritic ice formation, called the dendritic ice formation process. This process begins at the occurrence of nucleation, when the water temperature is T_n . Once nucleation occurs, a thin slice of dendritic ice, as shown in Fig. 2(c), spreads rapidly from the nucleation site down toward the center region of the cylinder; in the meanwhile, it also grows down along the cold boundary layer region adjacent to the inner cylinder surface. Latent heat released by dendritic ice enables the supercooled water temperature to rise to the temperature T_m , (d), where ice and water can coexist inside the capsule. Once this equilibrium temperature is reached, the formation of dendritic ice ends. The duration of this process is very short, lasting only 1 to 5 seconds, depending on the degree of supercooling. In curve IV, the phase change doesn't happen and the water remains in a metastable state for an undetermined time without the formation of dendritic ice. The third stage involves the phase-change process, from the completion of ice crystals formation to the complete freezing of the water inside the capsule. This is called the latent heat thermal storage process. This process begins after the dendritic ice formation is finished. As indicated in Fig. 2(e), a thick ice layer starts to form from the inner surface of the capsule toward the cell center till the water is completely frozen (f). The last stage involves the process of the cooling of ice until it reaches the same temperature as that of the coolant temperature. This process is similar to the water sensible heat thermal storage process (g).

For the case presented in Fig. 1, as supercooling doesn't happen, the solidification process happens without the formation of dendritic ice in any stage. For the curves II and III, Fig. 2, stage 3 is nearly null (rapid phase change).

2. EXPERIMENTAL APPARATUS

The experimental apparatus, shown schematically in Figure 3, consists of a test section (1), an observing system (2), a cooling system (3) and (4), and a measurement and data logging system (5).

2.1. Test section.

This section contains the capsule to be analyzed. The walls are made of a 10 mm thick acrylic plate externally covered with a 25 mm thick insulation. A test section transversal cut is shown in the Figure 4. The diffuser is intended to homogenize the TF temperature in the test section. The temperature control is carried out by a constant temperature bath which receives the signals from a temperature sensor - RTD type PT-100. K type thermocouples were used for the circulating fluid temperature registration. Two flanges are installed in the vertical walls to facilitate the cylinder change. An overflow tank, working at atmospheric pressure, was installed to compensate the volume variation during the phase change. In the same figure, the cylindrical capsule, filled with the PCM, can be observed. K type thermocouples of 0,076 mm diameter, covered with Teflon, are also indicated. Their positions are in Fig. 5 and expressed in Table I. These thermocouples are used to register the temperature during the experiences. To define the

volume of the PCM, a sliding disk (movable in the axial direction) is used. The acrylic capsule is shown in Fig. 6.

2.2. Observing system

A digital camera (30 images per second), located inside a box, is used to register the exact instant of the nucleation and the growth of the ice. To avoid condensation, the space between the capsule and the camera's lens is filled with nitrogen, an inert gas that removes the humid air. The box is also insulated.

2.3. Cooling system

The cooling system can be seen in Fig. 3. It is composed of two constant temperature baths (CTB) (3), two reservoirs (4) and the transfer fluid (TF). The initial temperature for the tests is set at one CTB while the other CTB is set at the test temperature. The temperature control system is of the PID type (Proportional Integral Derivative) and it is able to maintain the temperature into a range of ± 0.05 °C with a refrigeration power of 800 W at 0 °C and 1000 W of electric power heater. The transfer fluid is an alcohol-water solution (50% in volume).

2.4. Measuring and data logging system

The measurements and storage of data are made by the data acquisition system and a personal computer (PC). The acquisition equipment, which communicates with the PC by the RS232 communication port, receives processes and transmits the temperature signals to PC for storage and posterior analysis.

3. EXPERIMENTAL PROCEDURE

The initial water temperature inside the capsule (25.0 °C) was imposed using a constant temperature bath (CTB). The cooling procedure starts by pumping the transfer fluid (TF) through the upper reservoir while its temperature is controlled by the second CTB. At this time the test section is empty at the initial temperature. When the desired test temperature is reached, the FT is addressed to the section test absorbing the initial thermal loads and passing later to the underneath tank. When the upper tank is empty, the flow of the CTB is addressed toward the test section. After each test, a pump impels the FT toward the upper reservoir for a new test. This procedure is carried out to maintain the test temperature constant along each test. A lapse of time shorter than 4 min is necessary for the FT temperature to reach stability. This lapse represents less than 2.5% of the total test time. See Δt in Fig. 7.

The duration of each test varies from 1 to 5 hours, depending of the test conditions and material of the capsule. If the nucleation doesn't happen within 5 hours, the test is interrupted. The data is acquired once a second. Uncertainties are presented in Table II.

3.1. Investigated parameters

The following parameters were investigated: supercooling and nucleation probability, cooling rate and temperature field for cylindrical capsules made of acrylic, PVC, brass and aluminum. All capsules have a 45 mm internal diameter and 1.5 mm wall thickness. Experiences were carried out with different temperatures of the transfer fluid (TF), varying from -2 to -10 °C, in steps of 2 °C. For each temperature of the FT, the procedure was repeated 20 times, with the same initial and boundary conditions.

4. RESULTS AND DISCUSSION

4.1 Effect of the cooling rate

The cooling rate is defined as the inner wall average temperature gradient evaluated from the start of supercooling until the nucleation, or,

$$CR = \frac{\sum_{i=1}^n CR_i}{n} = \frac{\sum_{i=1}^n \frac{(T_{IW_i} - T_{IW_{i-1}})}{\Delta t'}}{n}, \text{ or, } CR = \frac{SD}{\Delta t} \dots\dots\dots (1)$$

CR is the cooling rate in the internal wall

T_{IW_i} is the internal wall temperature

$\Delta t'$ is the time interval of acquisition data and n is the number of measurements.

Δt is the total supercooling time and the supercooling degree SD

SD is the supercooling degree

Figure 8 shows a test interrupted after 5 hours of supercooling without nucleation. The effect of the T_{TF} can be observed in Figs. 9 and 10. In both cases it is possible to observe the phenomenon of supercooling, but for bigger T_{TF} , the nucleation takes more time to occur. It was always observed.

A solidification process without supercooling is observed in Fig. 11. The phase change occurs exactly at T_m .

In Fig. 12, it is observed that the PCM starts supercooling (IW) and returns to T_m . It was caused, probably, by the convection due to the density inversion effect. After some time, the supercooling appears again and the nucleation takes place, starting the solidification process. The IW temperature in Fig. 13 shows a phenomenon defined as

hypercooling (temperature in IW). When the nucleation occurs, the temperature rises to a value smaller than T_m and continues falling in the sensible stage.

Fig. 14 shows the supercooling period as a function of cooling rate and material. It is possible to see the great influence of the CR. Large values of this variable imply short periods of supercooling.

4.2 Effect of coolant temperature on supercooling and nucleation probabilities

Figs. 15 and 16, show, respectively, the supercooling and nucleation probability distribution curves, under different conditions of coolant temperatures, varying from -2°C to -10°C , for pure water, contained in the different capsules.

$$N_s = \frac{\text{number of observed supercoolings}}{\text{total number of test}}, \quad N_F = \frac{\text{number of nucleations}}{\text{total number of test}} \dots\dots\dots(02)$$

N_s and N_F are the supercooling and nucleation probabilities.

It is possible to see that the supercooling probability increases for bigger T_{TF} . For T_{TF} -2 and -4°C , this probability was 100%, independent of the material of the capsules. The acrylic capsules present bigger probability of supercooling, probably due to its low thermal conductivity. On the other hand, the aluminum capsule presents more cases of supercooling than the PVC capsules. The reason for that could be its roughness and should be well investigated. The probability of nucleation is presented in Fig. 16 and shows that for high thermal conductivity materials, the nucleation occurs more frequently. It can be explained by the stronger convection inside the capsules, facilitating the starting of the freezing process.

4.3 Nucleation and solidification process

The nucleation process inside the acrylic capsule for $T_{TF} = -8\text{ }^{\circ}\text{C}$ can be observed in Fig. 17. The left hand side of the figure presents the pictures captured along the test. On the right hand side a schematic representation of the phenomenon is presented. The entire process takes about 3 seconds. In the first image the PCM is supercooled at $-8\text{ }^{\circ}\text{C}$ and, for this particular case, the nucleation starts after 3500 seconds from the beginning of the cooling process. The sequence shows the development of scattered thin dendrites distributed inside the capsule. Figure 18 shows the continuation of the same case. After the nucleation, solid ice grows from the wall. This process is slower than the nucleation one and takes approximately 4.6 hours to be completed. For each image of the sequence in Fig. 18 the correspondent instant of time is shown in minutes. Two different structures can be seen inside the capsule. A diffuse interface between the solid ice and the solid dendritic structure regions is observed. Fig. 19 shows the images captured from the solidification process of the water without supercooling, for the aluminum capsule with $T_{TF} = -6^{\circ}\text{C}$. In this case the dendritic structure is not present and the interface is sharp and well defined. The total solidification process lasted 6.16 hours.

5. CONCLUSION

The supercooling phenomenon was experimentally investigated inside cylindrical capsules filled with pure water, utilized as Phase Change Material (PCM) for cool storage systems. Cylinders with 45 mm internal diameter and 1.5 mm wall thickness, made from four different materials (Acrylic, PVC, Brass and Aluminum) were investigated. The water supercooling period and the nucleation temperature were investigated for different transfer fluid temperatures. Characteristic curves of water

cooling processes in cylindrical capsules with or without supercooling effects were observed. Particular experiments were done, where continuous metastable states were observed, or cases of double supercooling phenomenon. It was verified that the supercooling probability increases for bigger T_{TF} values. For T_{TF} -2 and -4°C, the probability of supercooling was 100%, independent of the material of the capsule. Nucleation is more frequent in experiences with high thermal conductivity materials. When supercooling appears, dendritic ice accompanies the solidification process, as well as the presence of a kind of mushy region. In the cases without supercooling, the interface between the ice and the liquid water is well defined with no dendritic formation.

REFERENCES

1. S. L. Chen and T. Z. Lee. A study of the supercooling phenomenon and the freezing probability of water inside horizontal cylinders, International Journal of Heat and Mass Transfer, Volume 41, Issues 4-5, 3, Pages 769-783 (1998).
2. J. I. Yoon, C. G. Moon, E. Kim, Y. S. Son, J. D. Kim, T. Kato. Experimental study on the freezing of water with supercooled region in a horizontal cylinder. Applied Thermal Engineering 21, 657-668 (2001).
3. J.J. Milón and S. L. Braga, Spherical encapsulated cold storage, ICR 2003 –21st International Congress of Refrigeration, US, (2003).

Table I. Temperature sensors in the capsule.

Symbol	Description	Distance from the center line
TF	Transfer fluid	1,2 R
EW	External wall	-(R+z)
IW	Internal wall	-R
RMR	Right middle radius	+R/2
C	Center	0
LMR	Left middle radius	-R/2

R is the cylinder radius and z is the cylinder wall thickness

Table II. Uncertainties of measurements

Parameter	Uncertainty
Temperature	0,1 °C
Time	0,1 s
Length	0,1 mm

Figure Captions

Fig. 1. Stable solidification of water.

Fig. 2. Metastable solidification of water.

Fig. 3. Experimental apparatus schematic diagram: test section (1); observing section (2); cooling section: constant temperature bath (3) and reservoir (4), (5).

Fig. 4. Test section details.

Fig. 5. Test cylinder view.

Fig. 6. Capsule front view with thermocouples distribution.

Fig. 7. Temperature of the TF during a typical test.

Fig. 8. Temperature versus time, acrylic, $T_{FT} = -6\text{ }^{\circ}\text{C}$

Fig. 9. Temperature versus time, brass, $T_{FT} = -6\text{ }^{\circ}\text{C}$, $CR = 0,082\text{ C/min}$

Fig. 10. Temperature versus time, PVC, $T_{FT} = -8\text{ }^{\circ}\text{C}$, $CR = 0,214\text{ C/min}$

Fig. 11. Temperature versus time, brass, $T_{FT}=-8\text{ }^{\circ}\text{C}$

Fig. 12. Temperature versus time, PVC, $T_{FT}=-10\text{ }^{\circ}\text{C}$, $CR=0,556\text{ C/min}$

Fig. 13. Temperature versus time, aluminum, $T_{FT}=-10\text{ }^{\circ}\text{C}$, $CR=0,609\text{ C/min}$

Fig. 14. Supercooling period as a function of the cooling rate, different materials.

Fig. 15. Supercooling probability

Fig. 16. Nucleation probability

Fig. 17. Nucleation process: The left column shows the real image, the middle one the time, in seconds, and the right one the processed image. Acrylic with $T_{FT} = -8\text{ }^{\circ}\text{C}$.

Fig. 18. Solidification process: The left column shows the real image, the middle one the time, in minutes, and the right one the processed image. Acrylic with $T_{FT} = -8\text{ }^{\circ}\text{C}$

Fig. 19. Solidification process: The left column shows the real image, the middle one the time, in minutes, and the right one the processed image. Brass with $T_{FT} = -6\text{ }^{\circ}\text{C}$.

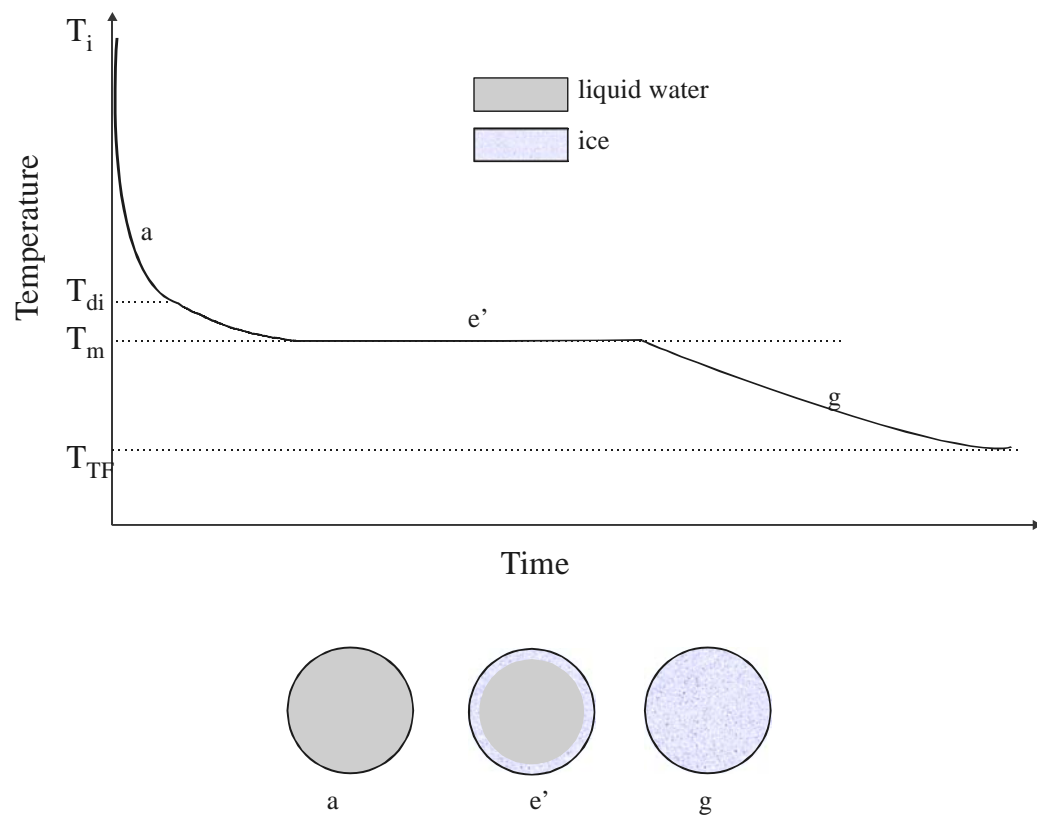


Fig. 1

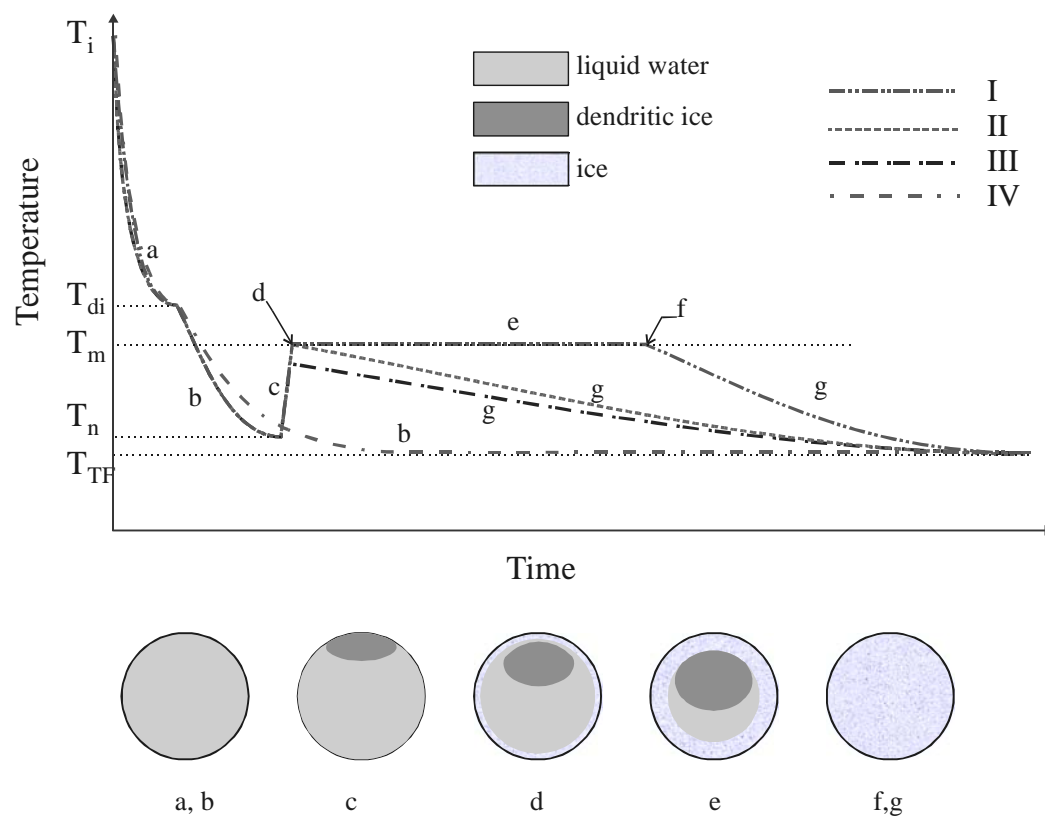


Fig. 2

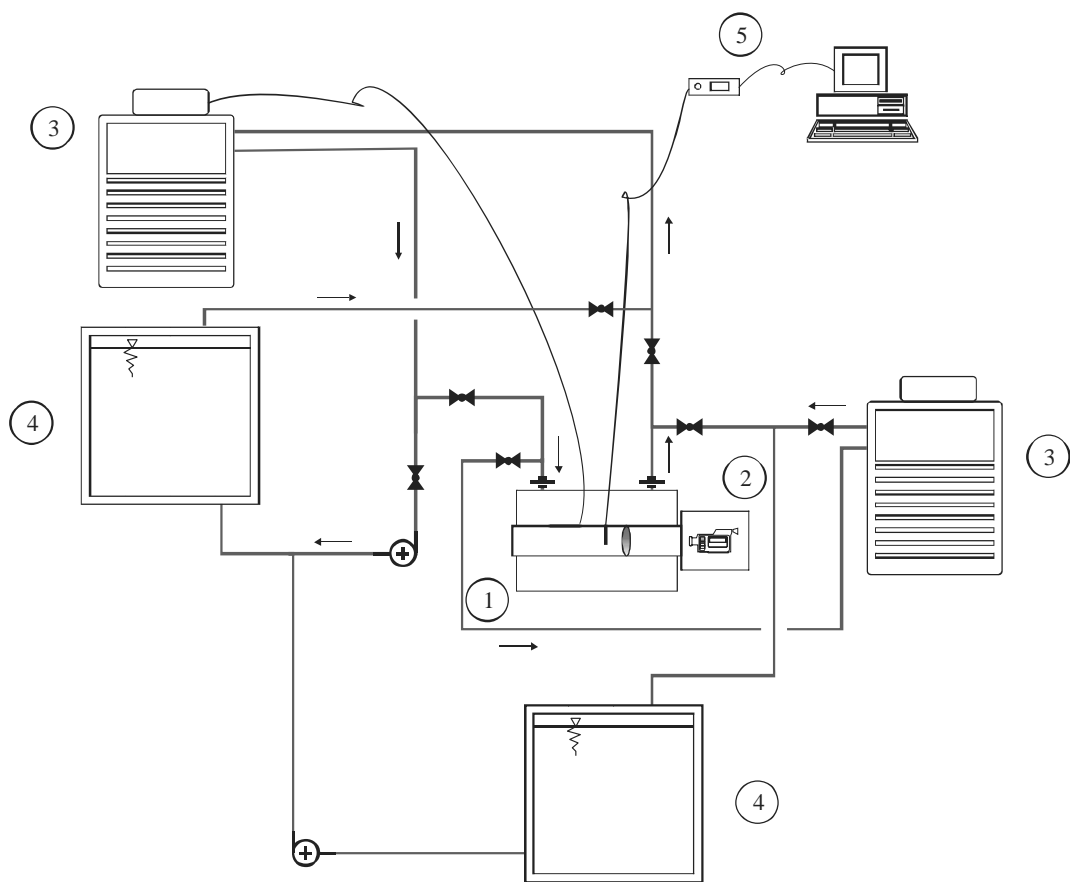


Fig. 3

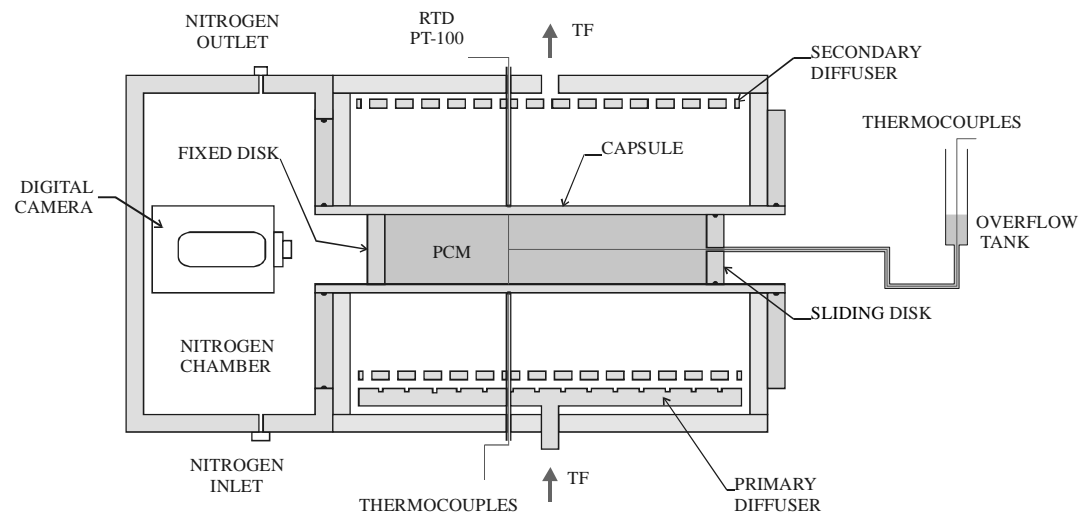


Fig. 4

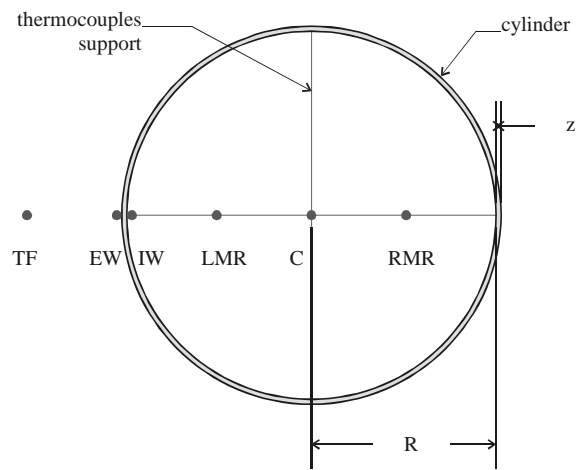


Fig. 5



Fig. 6

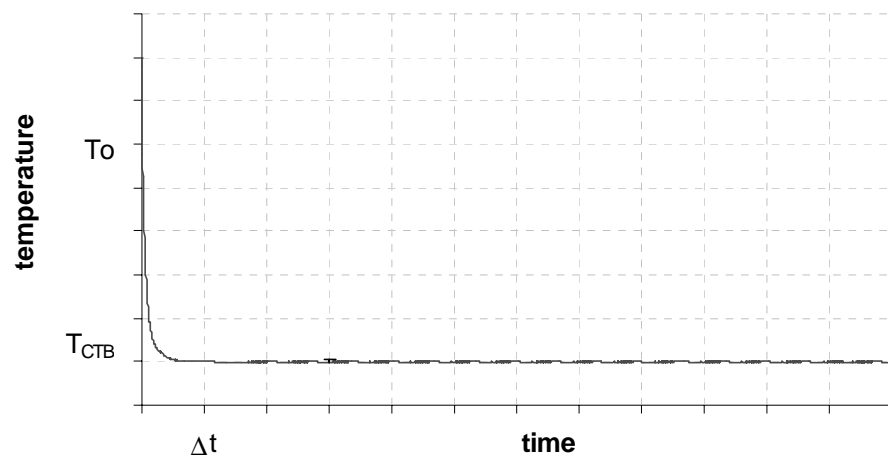


Fig.7

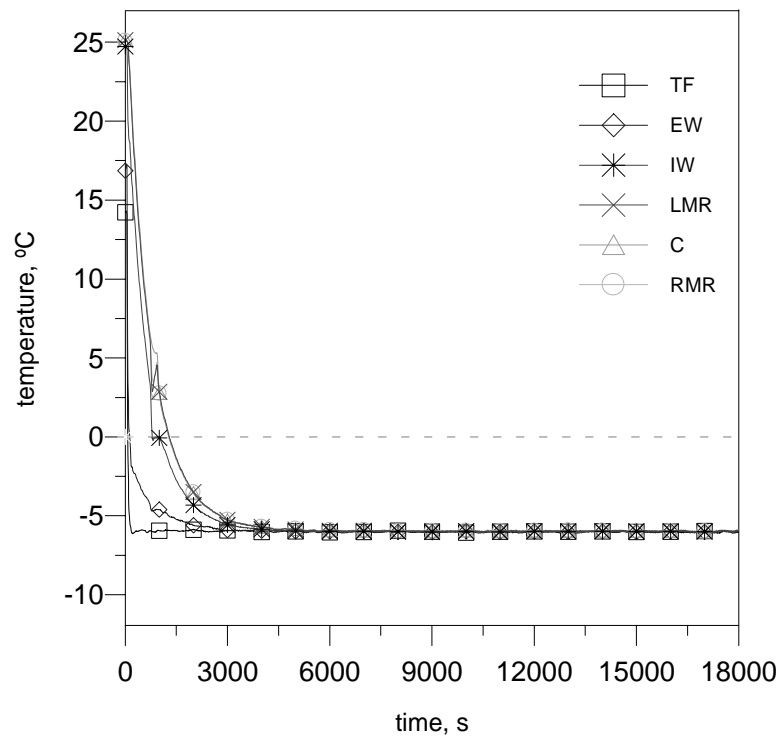


Fig. 8

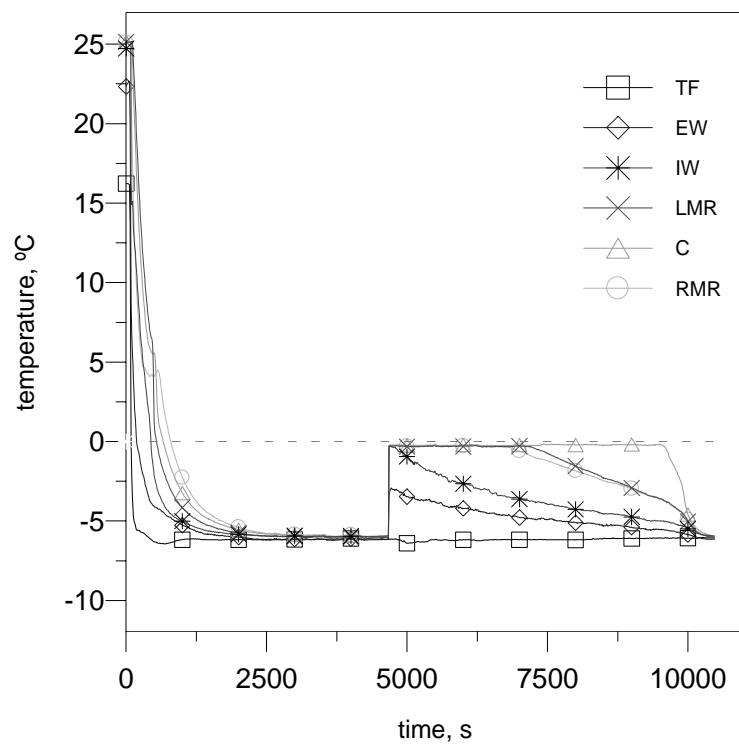


Fig. 9

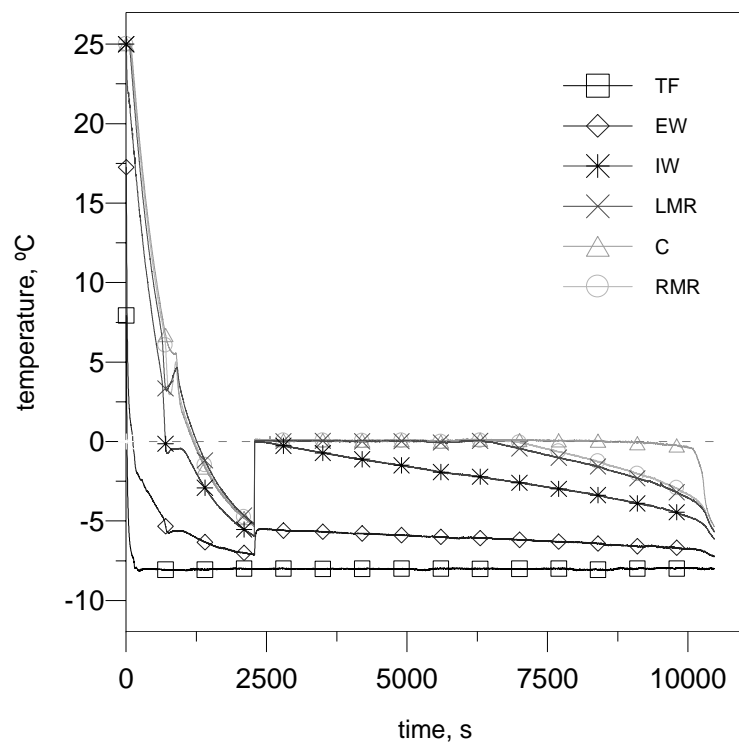


Fig. 10

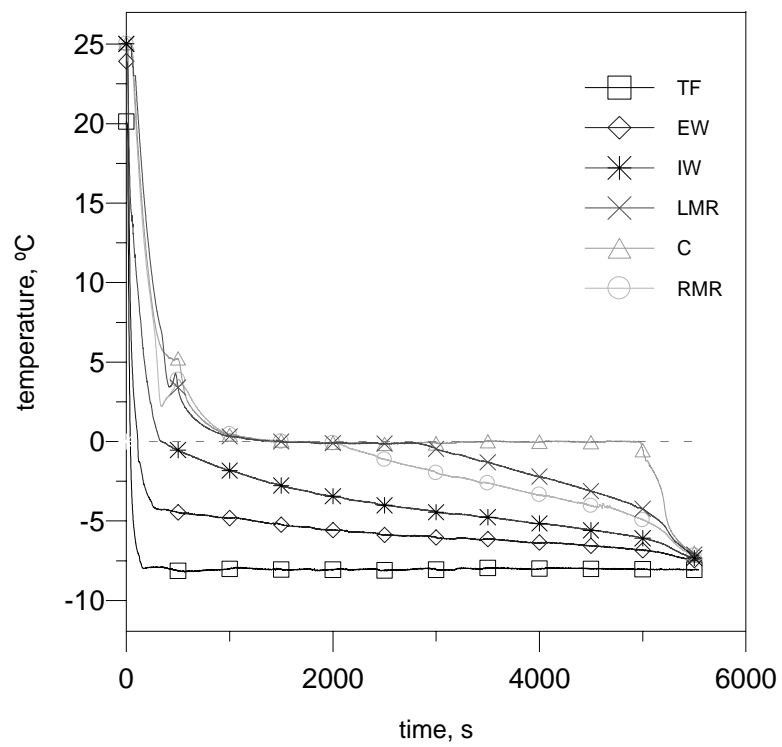


Fig. 11

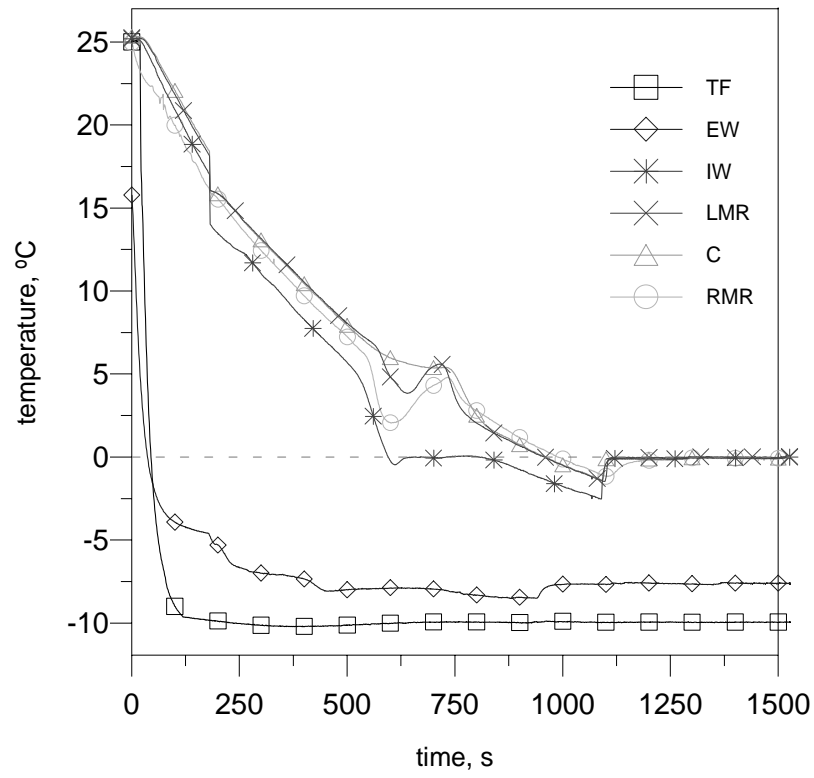


Fig. 12

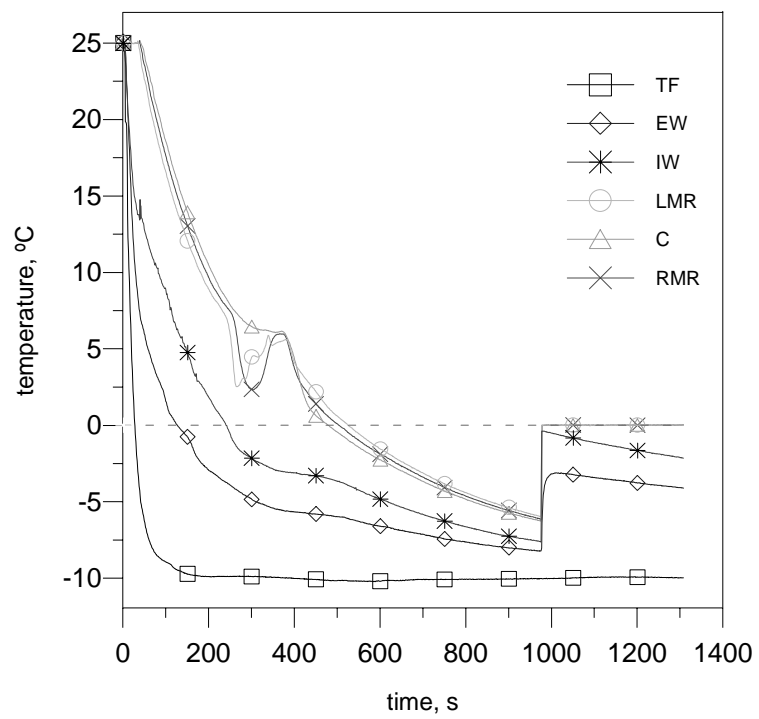


Fig. 13

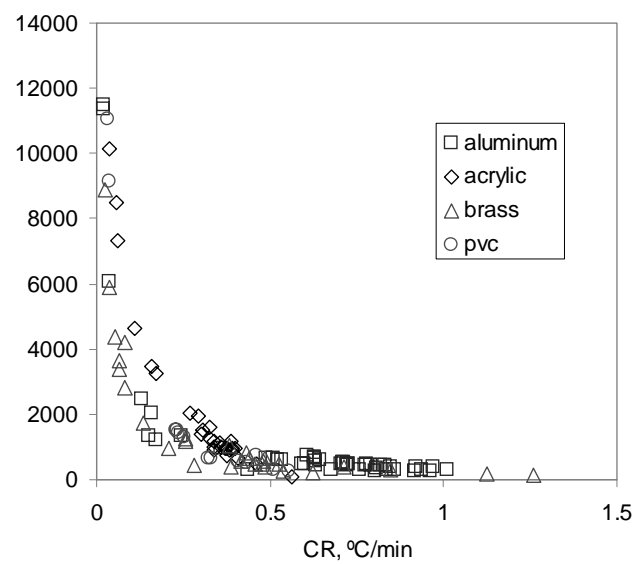


Fig. 14

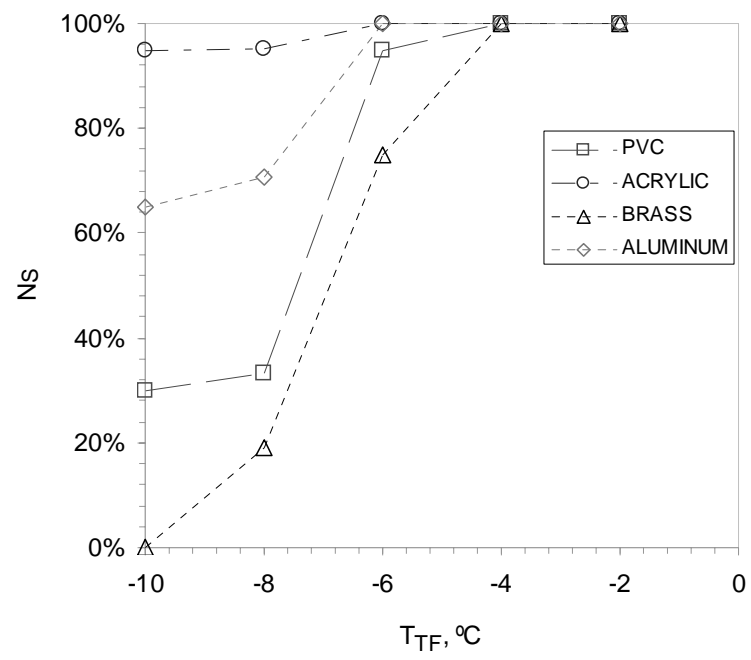


Fig. 15

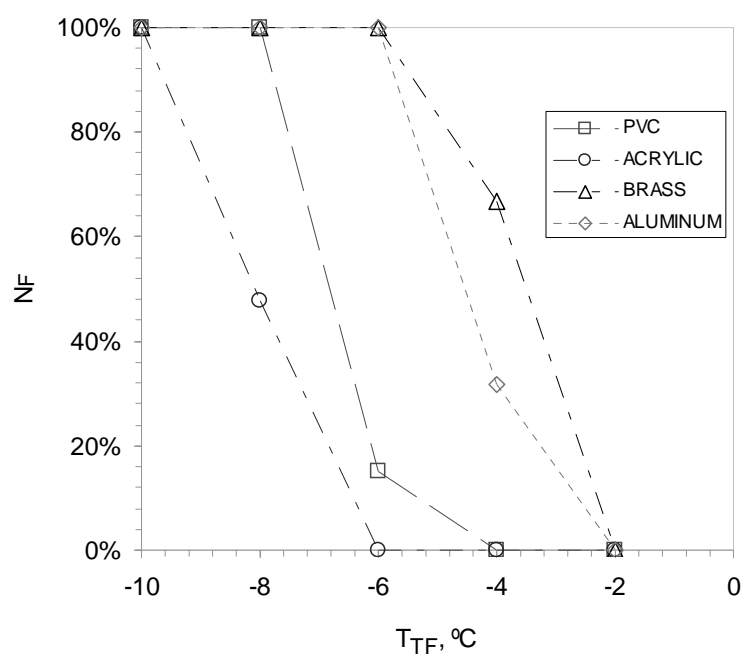


Fig. 17

Fig. 16

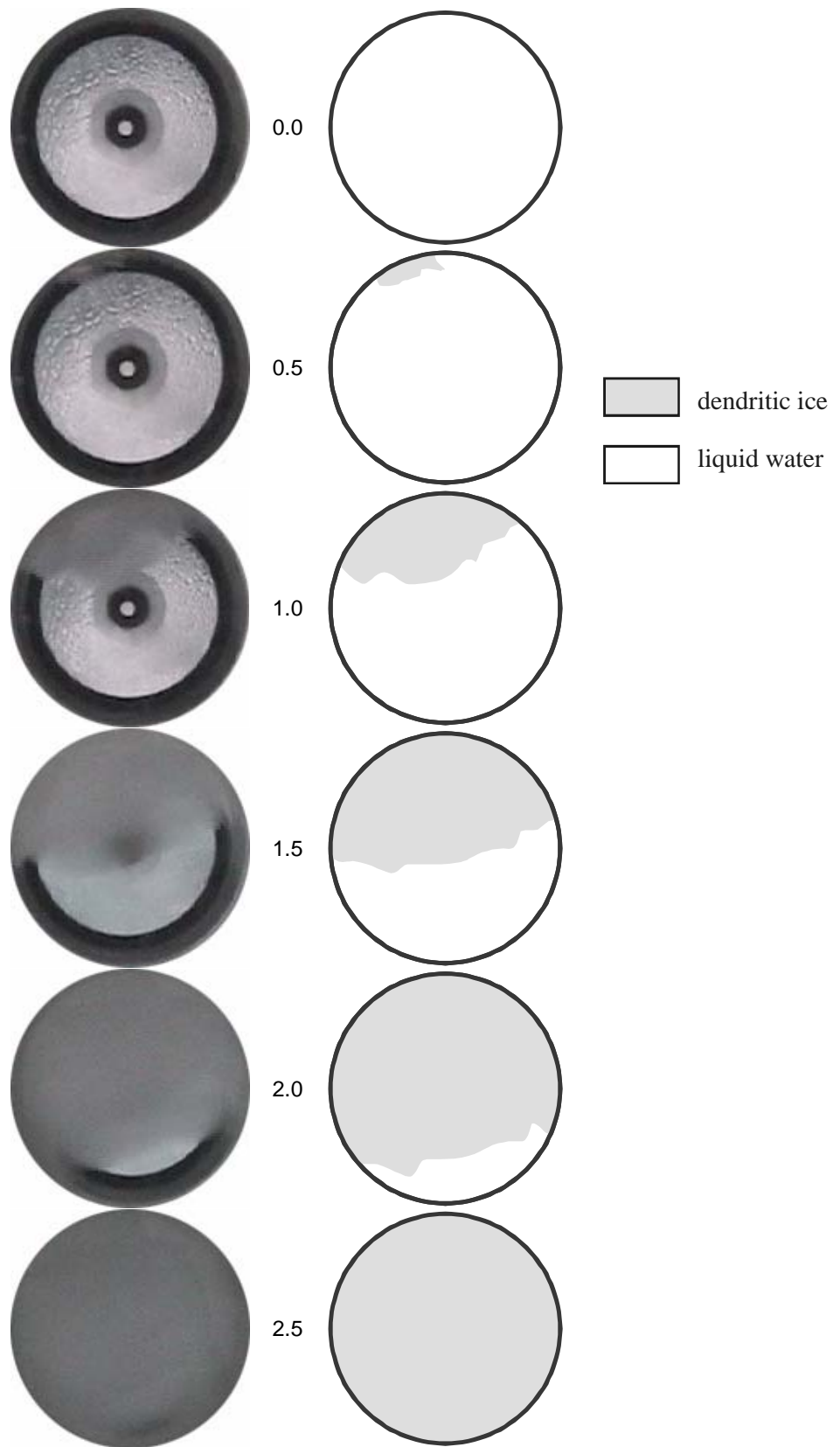


Fig. 17

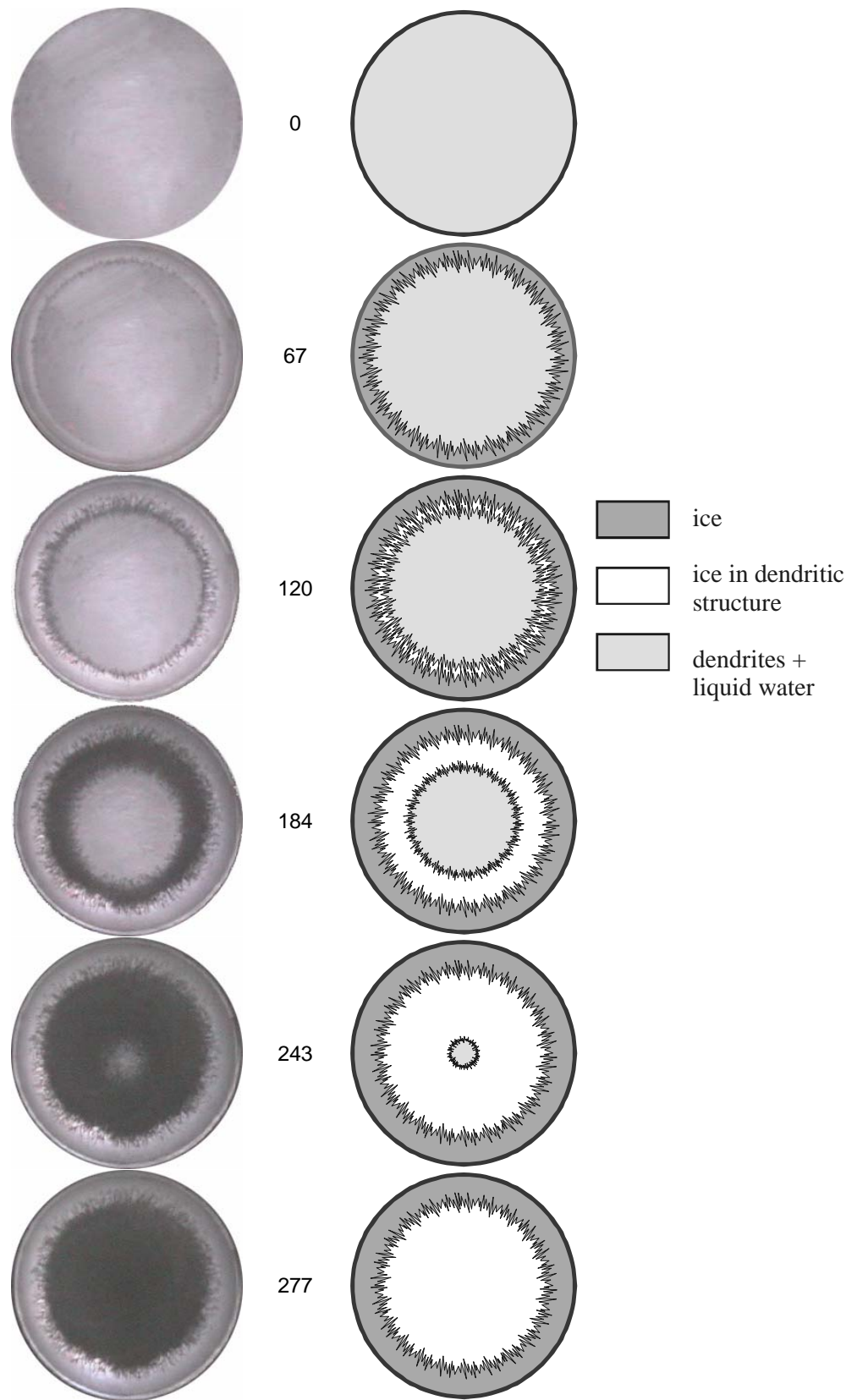


Fig. 18

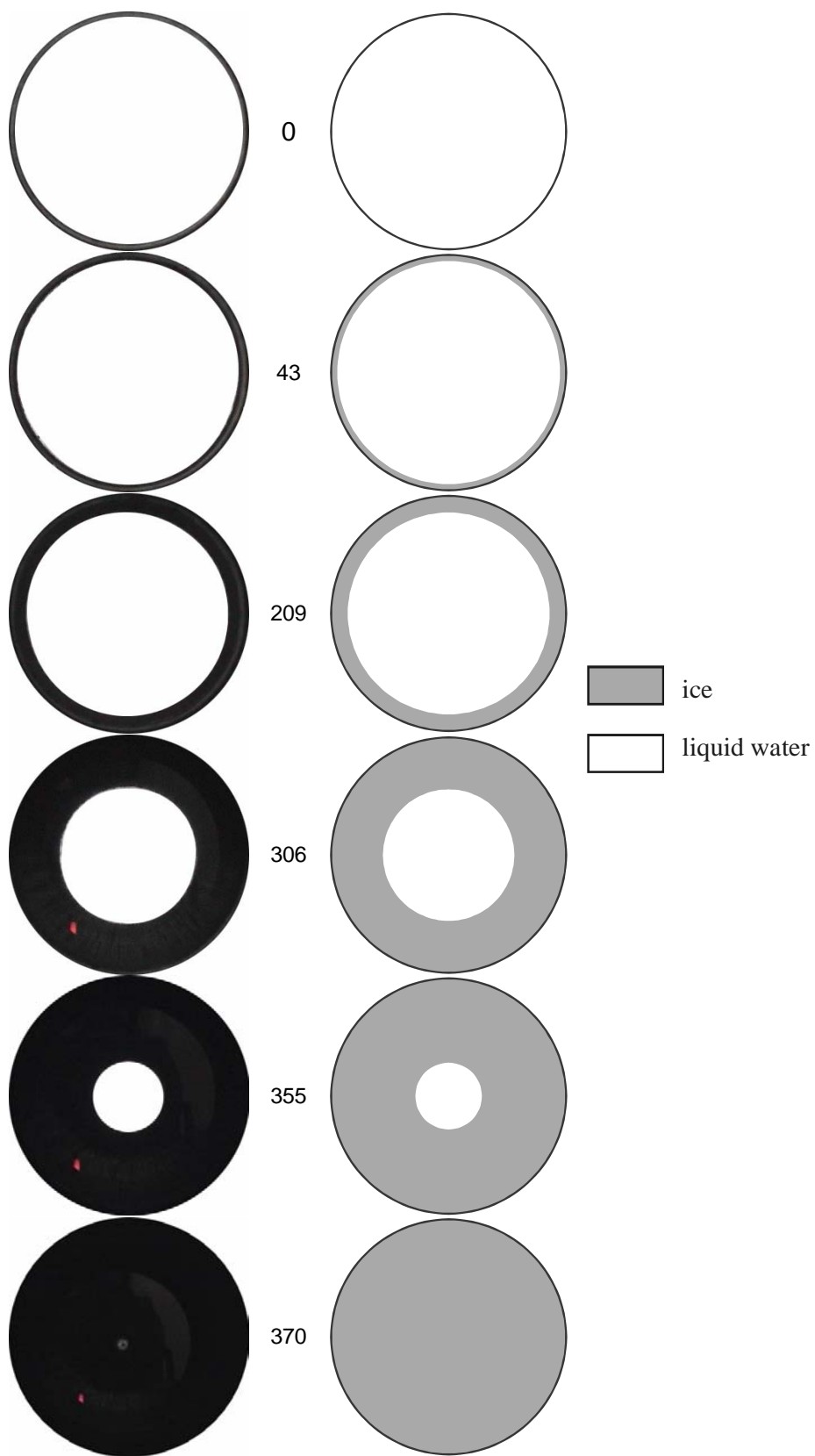


Fig. 19